EFFECT OF INTERNALLY MOUNTED HELICAL FINS ON THE SEPARATION PERFORMANCE OF A CYLINDRICAL GAS-SOLID CYCLONE SEPARATOR

Zeming FU [a], Huagen WU [a*], Baohua GAO [b], Mengtao LIANG [a], Guanghua WU [a], Shuo SHANG [c], Xin ZHANG [d], Hongye HUANG [a], and Siwei CHEN [a]

[a] School of Energy and Power Engineering, Xi'an Jiaotong University, Xi'an, China

[b] Shanghai Screw Compressor Co., Ltd, Shanghai, China

[c] School of Water and Environment, Chang'an University, Xi'an, China

[d] School of Resources Engineering, Xi'an University of Architecture and Technology, Xi'an, China

*Corresponding author: E-Mail: hgwu@mail.xjtu.edu.cn

In this study, an innovation was made by adding helical fins on the vortex finder of a cylindrical gas-solid cyclone separator, and the effect of this structural improvement on the separation performance was analyzed based on the flow field characteristics. The results show that both cyclones with and without helical fins exhibit a separation efficiency of almost 100 % for particles larger than 5 μm. As the inlet velocity increases, the effect of adding helical fins on the overall separation efficiency decreases, with a relative deviation of only 0.16 % at an inlet velocity of 27 m/s, while it becomes increasingly effective in reducing energy consumption, with a pressure drop of 25.33 %. The mechanism of the overall performance improvement lies in the fact that the helical fins change the flow field distribution in the cyclone, where the turbulence intensity in the vortex finder is significantly reduced, the tangential velocity of the external vortex is decreased, and the pressure gradient is reduced. The purpose of this paper is to provide new ideas for the optimal design of the internal components of the cyclone separator.

Keywords: *cyclone separator; gas-solid separation; helical fins; vortex finder*

1. Introduction

Atmospheric particulate matter (PM) pollution, especially $PM_{2.5}$, has become a serious global problem that endangers human health and can even cause premature death [1, 2]. Industrial emissions are one of the main sources of $PM_{2.5}$, making the separation of dust particles from industrial exhaust gases a critical area of research [3]. Cyclone separators are widely used in industry as an important gas-solid separation equipment due to their simple structure, low operation and maintenance costs, and high separation efficiency [4].

Numerous studies have explored the impact of cyclone structure and geometric parameters on their separation performance, and the vortex finder is crucial and strongly influences the flow field characteristics and particle motion within the cyclone [5, 6]. The effects of vortex finder diameter,

insertion depth, and shape have been widely investigated and confirmed by related research [5, 7, 8]. Researchers have attempted new design modifications in the vicinity of the vortex finder. The vortex finder with sidewall slotted gaps (SVF) was initially proposed by Xiong et al. [9] and evaluated through numerical and experimental investigations. Additional studies by other scholars have confirmed the potential industrial applications of cyclone separators with SVF [10-12], demonstrating improved performance compared to conventional vortex finders. Pei et al. [13] modified the local flow field of the vortex finder by adding a metal cross-shaped vane, and found that the cyclone with the modified vortex finder showed a significant reduction in pressure drop of 16.41 %, along with a slight increase in separation efficiency of 0.64 %. Misiulia et al. [14] found that the use of a deswirler on a vortex finder can reduce the total pressure drop by up to 32 %, depending on the location of the deswirler. Several deswirler designs have been developed and studied, demonstrating that their installation can improve separation efficiency and reduce pressure drop. Zhou et al. [15] improved flow field performance by adding spiral guide vanes to the vortex finder, indicating that an increase in the number of vanes led to a higher tangential velocity and collection efficiency. An optimal guide vane configuration can reduce airflow rotation in the vortex finder and lower energy dissipation, further enhancing separation efficiency. Helical fins are a specialized internal component that has received little attention. Dasar and Patil [16] examined the effects of three different cross-sectional helical fins affixed to the inner wall of the outer cylinder of a conventional Stairmand cyclone. They found that the separation efficiency was highest for the helical fins with a triangular cross-section. Yang et al. [17] conducted a follow-up investigation into the detailed separation process of triangular helical fins affixed to the inner wall of the cylinder, identifying their precise impact on separation performance and optimizing the structural parameters of the helical triangular fins. However, the impact of installing helical fins on the vortex finder, especially in cylindrical cyclones, has received little attention in the published literature. Unlike conventional Stairmand cyclones, cylindrical cyclones have a simpler and more cost-effective design with a lower pressure drop, albeit with lower separation efficiency. Cylindrical cyclones are commonly utilized in vertical multi-tube cyclone separation systems as secondary or tertiary cyclones [18].

In this study, we investigated the impact of adding helical fins on the vortex finder of a cylindrical cyclone on its flow field characteristics and separation performance through numerical simulation. Our findings are expected to provide valuable insights into the optimal design of internal components for cyclones.

2. Numerical simulation

2.1. Geometric model

In order to simulate the impact of helical fins on flow field distribution and separation performance, a cylindrical gas-solid cyclone separator was designed as the foundation. The dimensions of the cyclone body closely resemble the design proposed by Gao et al. [18]. The difference is that we adjusted the proportions of the main parameters vortex finder diameter (D_r) and cylindrical body height (H) to make it more similar to a conventional Stairmand cyclone separator. The structure of the cylindrical gas-solid cyclone and helical fins used in this study is shown in Fig 1, and the relevant dimensions of the geometry are shown in Tab 1.

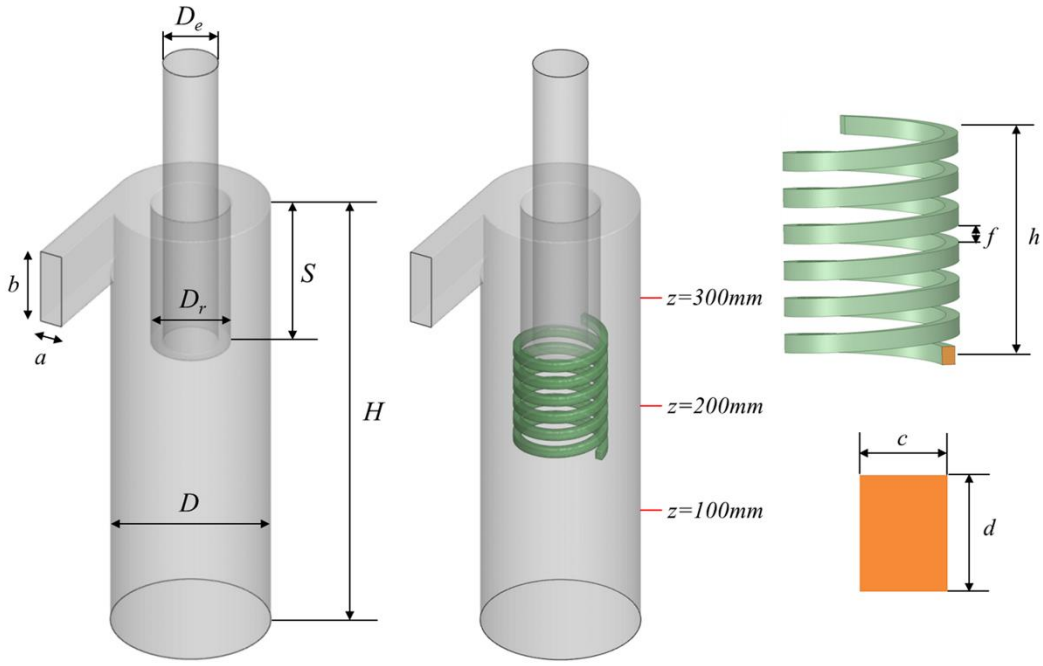

Figure. 1. Schematic of the structure of cyclones and helical fins.

Table 1. Geometrical dimensions of the geometric models.

Geometric parameter	Dimension (mm)
Entrance width, *a*	19.5
Entrance height, *b*	65
Cylinder diameter, *D*	130
Vortex finder diameter, D_r	65
outlet diameter, D_e	45
Cylindrical body height, *H*	390
Vortex finder height, *S*	130
helical fin height, *h*	88
helical fin pitch, *f*	8
Square section width, *c*	6
Square section Height, *d*	8

2.2. Mathematical models

The gas in a cyclone separator is usually considered incompressible. The motion of the continuous phase is determined by solving the continuity and momentum equations, which are expressed according to the Navier-Stokes equations as follows:

$$\frac{\partial \overline{u_i}}{\partial x_i} = 0 \tag{1}$$

$$\frac{\partial \overline{u_i}}{\partial t} + \overline{u_j}\frac{\partial \overline{u_i}}{\partial x_j} = -\frac{1}{\rho}\frac{\partial \overline{p}}{\partial x_i} + \nu\frac{\partial^2 \overline{u_i}}{\partial x_j \partial x_j} - \frac{\partial}{\partial x_j}\overline{u_i' u_j'} \tag{2}$$

where $\overline{u_i}$ denotes mean velocity; $\overline{p}$ is mean pressure; ρ and ν are density and kinematic viscosity, respectively; $\overline{u_i' u_j'}$ denotes Reynolds stress tensor.

The Reynolds Stress Model (RSM) and Large Eddy Simulation (LES) based on the RANS method are widely used in numerical studies of cyclones. The RSM shows good predictive capability by considering the effects of rotation, vorticity, high streamline curvature and rapid changes in strain rate. Compared with LES, the RSM model can significantly reduce the number of grids and

computational time while balancing prediction accuracy and computational cost [19, 20]. Therefore, the RSM model is used to solve the turbulent flow problem in the continuous phase. The Reynolds stress transfer equation is expressed as:

$$\frac{\partial}{\partial t}(\rho \overline{u_i' u_j'}) + \frac{\partial}{\partial x_k}(\rho u_k \overline{u_i' u_j'}) = D_{T,ij} + P_{ij} + \varphi_{ij} + \varepsilon_{ij} + S \tag{3}$$

The turbulent diffusion term, stress generation term, pressure strain term and dissipation term are:

$$D_{T,ij} = -\frac{\partial}{\partial x_k}[\rho \overline{u_i' u_j' u_k'} + \overline{p(\sigma_{jk} u_i' + \sigma_{ik} u_j')}] \tag{4}$$

$$P_{ij} = -\rho\left(\overline{u_i' u_k'}\frac{\partial \overline{u_j}}{\partial x_k} + \overline{u_k' u_j'}\frac{\partial \overline{u_i}}{\partial x_k}\right) \tag{5}$$

$$\varphi_{ij} = \overline{p\left(\frac{\partial u_i'}{\partial x_j} + \frac{\partial u_j'}{\partial x_i}\right)} \tag{6}$$

$$\varepsilon_{ij} = -2\rho\nu\overline{\frac{\partial u_i'}{\partial x_k}\frac{\partial u_i'}{\partial x_k}} \tag{7}$$

Particles are considered as discrete phases and the volume fraction is generally well below 10 %. It is reasonable to ignore the particle interactions and particle effects on the airflow at low particle concentrations. According to Newton's second law to control the motion of particles, the equation is expressed as:

$$\frac{du_p}{dt} = F_D(u - u_p) + \frac{v_p^2}{r_0} \tag{8}$$

$$\frac{dv_p}{d_t} = F_D(v - v_p) - \frac{u_p v_p}{r_0} \tag{9}$$

$$\frac{dw_p}{dt} = F_D(w - w_p) - g \tag{10}$$

where u_p, v_p, w_p denote the particle velocity in the x, y, z directions, and the drag force F_D is defined as:

$$F_D = \frac{18\mu}{\rho_p d_p^2}\frac{C_D \mathrm{Re}}{24} \tag{11}$$

$$\mathrm{Re} = \frac{\rho d_p |\, u_p - u|}{\mu} \tag{12}$$

where ρ_p is the particle density and d_p is the particle diameter. C_D is the drag coefficient calculated as:

$$C_D = a_1 + \frac{a_2}{\mathrm{Re}} + \frac{a_3}{\mathrm{Re}^2} \tag{13}$$

where a_1, a_2 and a_3 denote the constants.

In addition, the particle dispersion is strongly influenced by turbulent diffusion. The Discrete Random Walk (DRW) and Random Eddy Lifetime (REL) model were chosen to consider the effect of

turbulence on particle dispersion [6].

2.3. Grid independence

A hybrid mesh approach was used in this study due to the complex structure of helical fins, consisting of an unstructured tetrahedral mesh around the helical fins and a structured hexahedral mesh for the rest of the domain, as shown in Fig. 2(a). To ensure grid independence in the simulation, the tangential velocity of the cyclone fitted with fins at z = 100 mm was calculated using three grid levels with 466409, 631132, and 775680 cells, respectively. As shown in Fig. 2(b), the results for the three different grids are very close with an average relative error of less than 2.6 %, indicating that grid independent results can be achieved for all grids. The level with the highest number of grids was selected to ensure the best simulation results.

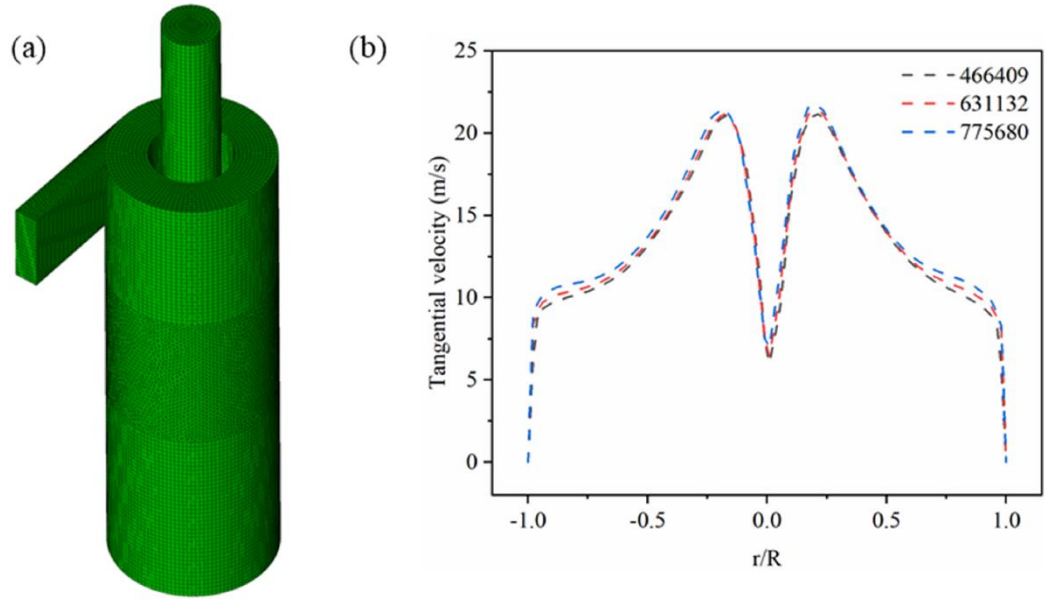

Figure. 2. (a) Grid representations; (b) Tangential velocities of the three grid levels at z = 100 mm.

2.4. Boundary conditions and simulation scheme

The velocity inlet was chosen as the inlet boundary condition with an inlet velocity of 12-27 m/s. Air is used as a continuous phase with a density of 1.225 kg/m^3 and a dynamic viscosity of 1.7894×10^{-5} Pa s. The hydraulic diameter and turbulence intensity can be calculated as:

$$I = 0.16\left(Re\right)^{-1/8} \tag{14}$$

$$D_H = 4A / L \tag{15}$$

where *Re* is the Reynolds number, A is the inlet area, and L is the inlet perimeter. The outlet surface of the vortex finder was set as the pressure outlet. Both the helical fins and the wall surface adopted the standard wall function and no-slip boundary condition. The particles were assumed to be spherical particles with a density of 2650 kg/m^3 and injected from the inlet at the same velocity as the continuous phase. The separation efficiency of cyclones is very high for particles larger than 10 μm, so

this study focused on particles smaller than 10 μm. The size of the particles follows a Rosin-Rammler distribution, with a mean particle diameter of 2.47 μm and a spread parameter of 4.31. The bottom surface was set as a trap, the exit surface of the vortex finder was set as an escape. For particle-wall collisions, the restitution coefficients for the normal (e_n) and tangent (e_t) directions are [21]:

$$e_n = 1 - 0.0218\alpha + 0.0002\alpha^2 \tag{16}$$

$$e_t = 0.7829 - 0.0041\alpha + 0.00004\alpha^2 \tag{17}$$

where α is the impact angle. The spatial discretization methods used are summarized in Tab 2. Transient runs were performed for the flow field with a time step of 0.0001 s and a convergence criterion of 1×10^{-5} for all solution variables.

Table 2 Numerical schemes for this study.

Numerical setting	Scheme
Pressure discretization	PRESTO!
Pressure velocity coupling	SIMPLEC
Momentum discretization	QUICK
Turbulent kinetic energy	Second-order upwind
Turbulent dissipation rate	Second-order upwind
Reynolds stress	First-order upwind

2.5. Model validation

To validate the numerical method of this study, the simulation results were compared with the experimental data in the literature [22, 23]. The simulations here were performed according to the exact geometric parameters in their experiments. As shown in Fig. 3, the simulation data are consistent with the experimental test data and can accurately reflect the flow of the flow field and the motion of the particles.

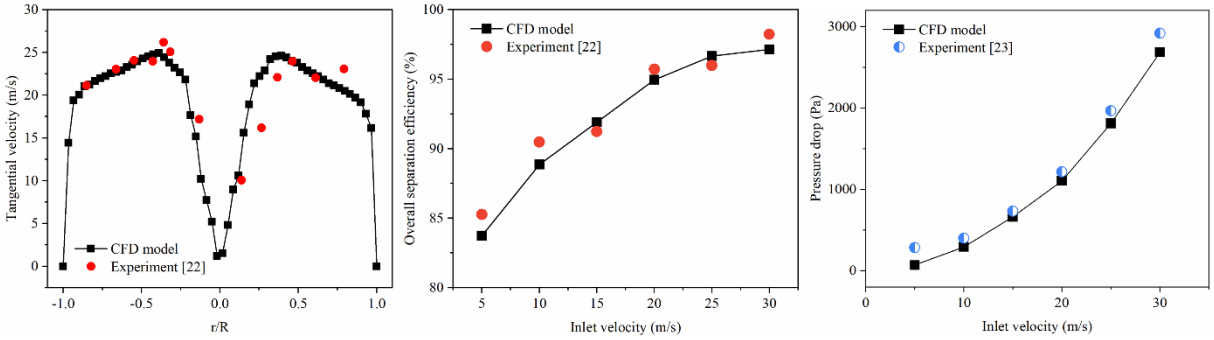

Figure. 3. Comparison of simulated and experimental data.

3. Results and discussion

3.1. Tangential velocity field

The transient and time-averaged flow characteristics of the cyclone separator with and without helical fins were compared. Since the influence of the inlet Reynolds number on mean and turbulence statistics was proven negligible [24, 25], we selected the simulation results with an inlet velocity of 15m/s as a representative for analyzing the flow field characteristics. In the cyclone separator, a

strongly rotating turbulent flow field is generated. The tangential velocity plays a crucial role in particle separation, the higher the tangential velocity, the greater the centrifugal force acting on the particles. Figure 4 illustrates a comparison of the tangential velocity distribution, at various cross-sections. It is evident that the distribution of tangential velocity takes the form of a Rankine vortex structure, which comprises an external quasi-free vortex and an internal quasi-forced vortex [26]. The maximum tangential velocity occurs at the interface of the inner and outer vortices in the separation space and near the inner wall of the vortex finder. The addition of helical fins to the vortex finder has little effect on the tangential velocity of the inner vortex and some effect on the tangential velocity of the outer vortex. At z=100 mm, a decrease in the tangential velocity of the outer vortex is observed after the installation of the helical fins. At z=200 mm, the overall decrease in the tangential velocity of the outer vortex is observed, but there is a slight increase near the wall due to the presence of the helical fins, which narrow the annular separation space here. At z=300 mm, the tangential velocity distribution is very close, and the inlet velocity has a dominant effect on the tangential velocity near the top of the cyclone, while the helical fins have less effect on the upper flow field.

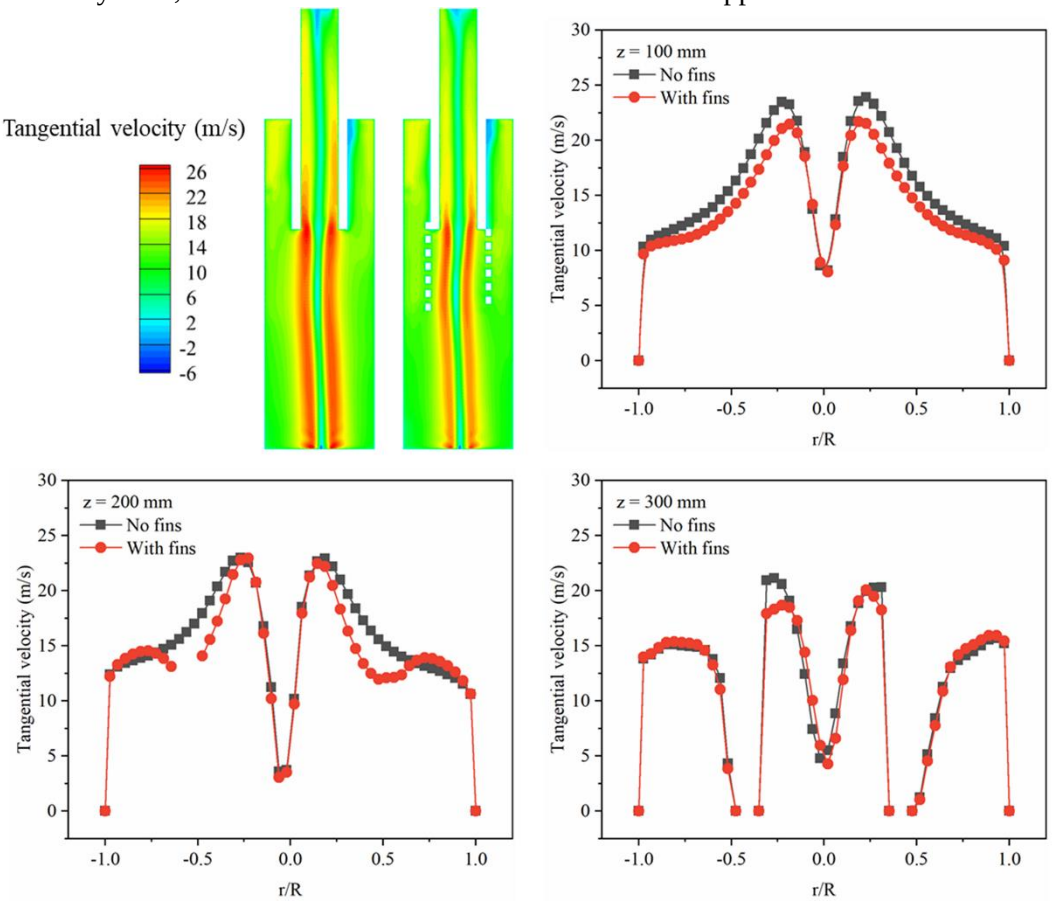

Figure. 4. Comparison of tangential velocity distribution at v_{in} = 15 m/s.

3.2. Pressure

Comparing the difference in static pressure distribution between the two cyclones helps to understand the variation in pressure drop. Figure. 5 shows the distribution of the static pressure, which has a good symmetry. The static pressure decreases along the radial direction from the wall to the center in the main separation space, with little change in the axial position. This is due to the acceleration of the gas from the external vortex to the internal vortex and the conversion of the static

pressure to dynamic pressure, resulting in a decrease. Due to the radial pressure gradient and the exit tube discharge driven by the upward axial velocity, many smaller particles enter the inner vortex under resistance. The addition of helical fins on the vortex finder results in a decrease in the pressure gradient of the external vortex. This reduction can be attributed to a decrease in tangential velocity. As the airflow approaches the center of the cyclone, the kinetic energy of the vortex is transformed into potential energy, leading to a subsequent reduction in the pressure gradient.

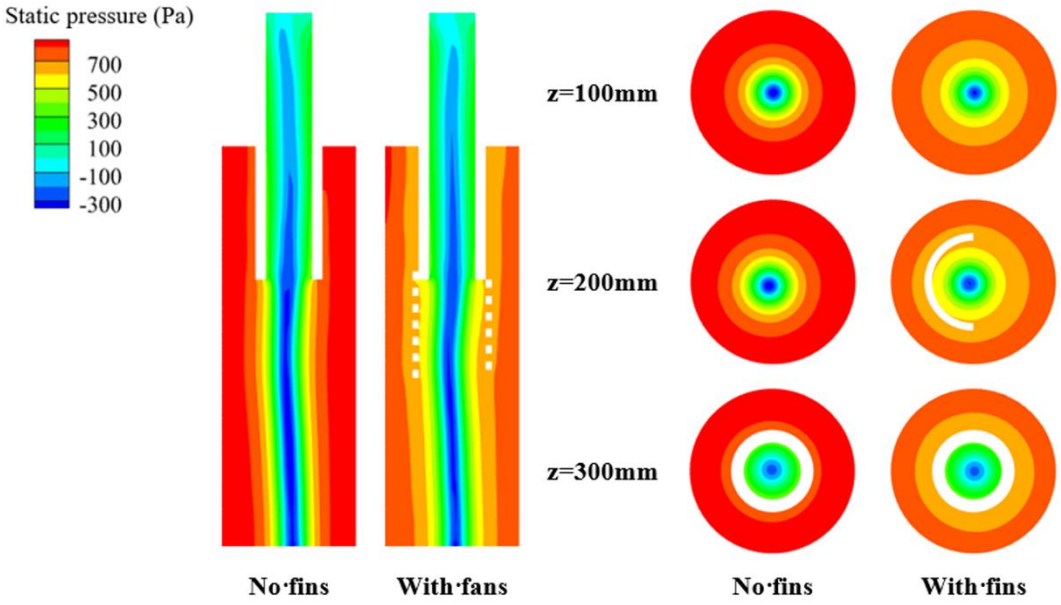

Figure. 5. Comparison of static pressure distribution at v_{in} = 15 m/s.

3.4. Turbulence intensity

Turbulence is an important factor in cyclone separators because it affects the efficiency and performance of the separation process. Figure. 6 shows the turbulence intensity contours for the two cyclones at an inlet velocity of 15 m/s. The highest turbulence intensity values are located inside and below the vortex finder, while the lowest turbulence intensity occurs near the bottom of the cyclones. This implies that the region around the vortex finder has strong turbulent motion, while the bottom of the cyclones has relatively stable flow. It is evident that the addition of helical fins reduces the turbulence intensity in the vortex finder and weakens the turbulent motion compared to the separator without helical fins. The addition of helical fins on the vortex finder disrupts the coherence of the vortex, leading to vortex fragmentation and dissipation of turbulent kinetic energy into smaller scales of motion. This results in a reduction of turbulence intensity in the vortex finder. This is similar to the findings of Zhang et al. [3]. The decrease in turbulence intensity also explains the decrease in tangential velocity and the decrease in pressure gradient.

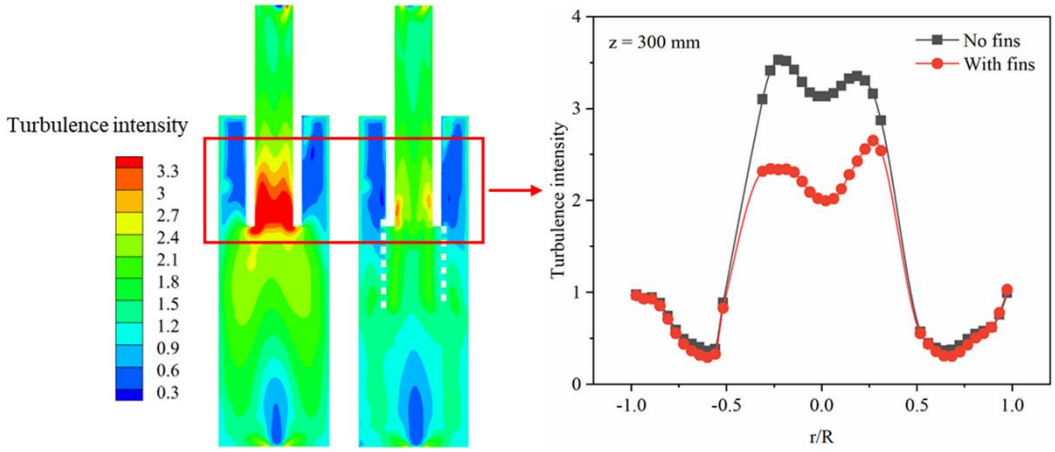

Figure. 6. Comparison of turbulence intensity distribution at v_{in} = 15 m/s.

3.5. Separation performance

The performance of a cyclone is mainly evaluated by two parameters: separation efficiency and pressure drop, with the former representing the separation capacity and the latter reflecting the energy consumption. The goal of structural improvement is to enhance the separation efficiency and reduce the pressure loss, which is challenging to achieve solely by altering the geometry. Therefore, achieving a balance between these two parameters is typically a crucial consideration. The pressure drop can be determined by calculating the difference between the average pressure values at the inlet and the outlet. The separation efficiency can be calculated by monitoring the particle mass at the inlet and the outlet and is calculated using the following formula:

$$\eta = (1 - \frac{m_o}{m_i}) \times 100\% \tag{16}$$

where η is separation efficiency, m_o and m_i are the mass of the particles escaping from the outlet and entering from the inlet.

The inlet velocity is a significant operating parameter that affects cyclone performance, and both pressure drop and separation efficiency are greatly influenced by it. Figure. 7 shows the pressure drop and overall separation efficiency of the two cyclones at different inlet velocities. At the same inlet velocity, the cyclones with helical fins have a lower pressure drop. With the increase of the inlet velocity, the pressure drop of two cyclones increases exponentially, which is consistent with Hoffman's theory [27]. However, the growth rate of pressure drop is significantly lower for the separator with helical fins. Compared with the original separator, the pressure drop of the separator with helical fins is reduced by 5.25 % at a low inlet velocity of 12 m/s. The reduction rate increases as the inlet velocity increase and reaches 25.33 % at a high inlet velocity of 27 m/s. This indicates that the helical fins on the vortex finder can significantly reduce the pressure loss of the cyclone for a high inlet velocity. The overall separation efficiency decreases at inlet velocities ranging from 12-21 m/s after adding helical fins. The decrease in the tangential velocity of the outer vortex is the main reason for the decrease in overall separation efficiency. The overall separation efficiency increases with increasing inlet velocity, but there is a marginal decreasing effect. This means that the effect of inlet velocity on separation efficiency decreases at higher inlet velocities, which is consistent with the theoretical model proposed by Avci and Karagoz [28]. This is due to the fact that excessive inlet

velocity will cause particles to bounce and larger particles will be entrained in the upward vortex to escape through the precessing vortex core [29], negatively impacting separation efficiency improvement.

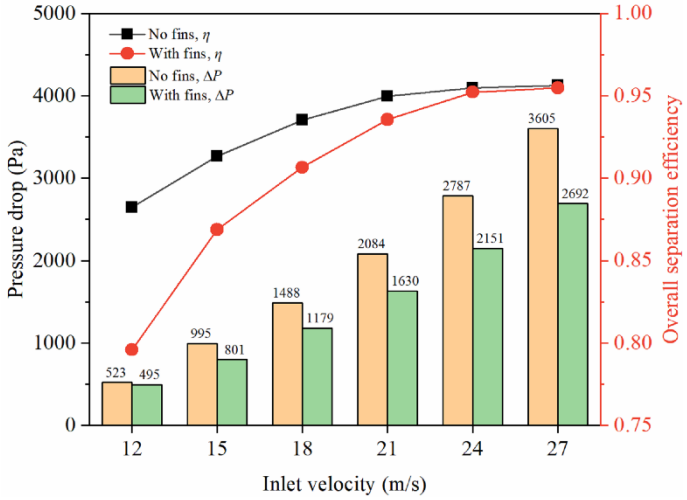

Figure. 7. The pressure drop and overall separation efficiency at different inlet velocities.

It is evident that the difference in the overall separation efficiency of the two cyclones becomes smaller as the inlet velocity increases, with a relative deviation of only 0.16 % at an inlet velocity of 27 m/s. This phenomenon can be explained by analyzing the variation in grade efficiency for different inlet velocities, as shown in Fig. 8. The separation efficiency is almost 100 % for particles above 5 μm. As the inlet velocity increases, the two grade efficiency curves are shifted to the left and become closer together, indicating a better separation of smaller particles, but there is only limited improvement in the separation efficiency of 1 μm particles. This is because increasing the inlet velocity generates a greater centrifugal force in favor of separation, but also causes turbulence and disturbances in the gas stream. Fine particles are strongly influenced by the turbulence to deviate from the separation trajectory and escape from the cyclone.

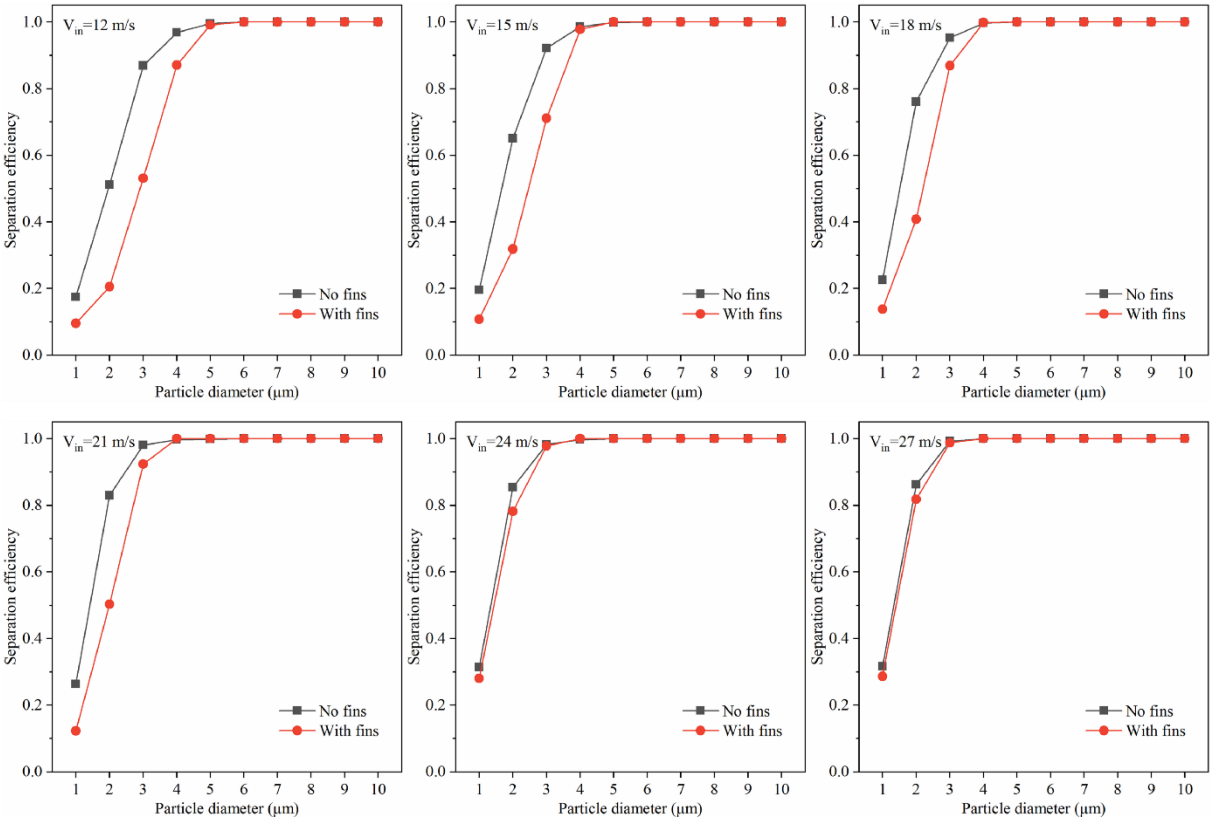

Figure. 8. The grade efficiency of two cyclones at different inlet velocities.

Cylindrical cyclones typically operate at higher gas velocities and are used to separate larger particle sizes. With the addition of helical fins, the small change in overall separation efficiency at high inlet gas velocities is almost negligible, and the significant reduction in pressure drop significantly reduces energy consumption. The addition of helical fins thus improves the overall performance of the cylindrical cyclone, which is a promising approach to optimizing the internal components of the cyclone.

4. Conclusions

In this paper, we propose the addition of helical fins on the vortex finder as an innovation, and analyze the effect of helical fins on the separation performance of cylindrical gas-solid cyclone based on the flow field characteristics through numerical simulation. This study provides an idea for optimizing the internal structure of the cyclone separator. Several noteworthy conclusions can be drawn as follows:

(1) The helical fins alter the flow field distribution in the cyclone separator, affecting its separation performance. By weakening turbulent motion in the cyclone, the helical fins reduce the turbulence intensity in the vortex finder. This results in a decrease in tangential velocity of the vortex outside the cyclone, leading to a lower pressure gradient. However, the helical fins have a lesser effect on the tangential velocity field inside the vortex finder and at the top of the cyclone.

(2) For particles larger than 5 μm, both cyclones with and without helical fins exhibit a separation efficiency of almost 100 %. As the inlet velocity increases, the effect of installing helical fins on the overall separation efficiency diminishes. At an inlet velocity of 27 m/s, the relative

deviation is only 0.16 %, which is negligible for cylindrical cyclones designed to separate larger particles.

(3) With an increase in inlet velocity, the significance of built-in helical fins in reducing pressure losses also increases. At a high inlet velocity of 27 m/s, the pressure drop is reduced by 25.33 %. This reduction in energy consumption leads to an improvement in overall performance.

Acknowledgements

Financial support from the National Natural Science Foundation of China (No. 50806055) is sincerely acknowledged.

References

[1] Zhang, X., *et al.*, Study of the water cleaning process by using CFD-DEM method: A case study of coarse filter material, *Thermal Science*. (2023), 00, pp. 88-88

[2] Zhang, X., *et al.*, Investigation of Indoor Air Quality and Staff Satisfaction in Underground Buildings in Xi'an, China, *Polish Journal of Environmental Studies*, 30. (2021), 4

[3] Zhang, Y., *et al.*, Heterogeneous condensation combined with inner vortex broken cyclone to achieve high collection efficiency of fine particles and low energy consumption, *Powder Technology*, *382*. (2021), pp. 420-430

[4] Gao, Z., *et al.*, Internal components optimization in cyclone separators: systematic classification and meta-analysis, *Separation & Purification Reviews*, *50*. (2021), 4, pp. 400-416

[5] Zhang, Z.-W., *et al.*, Simulation and experimental study of effect of vortex finder structural parameters on cyclone separator performance, *Separation and Purification Technology*, *286*. (2022), p. 120394

[6] Guo, M., *et al.*, Multi-objective optimization of a novel vortex finder for performance improvement of cyclone separator, *Powder Technology*, *410*. (2022), p. 117856

[7] Elsayed, K.,C. Lacor, The effect of cyclone vortex finder dimensions on the flow pattern and performance using LES, *Computers & Fluids*, *71*. (2013), pp. 224-239

[8] Tian, J., *et al.*, CFD simulation of hydrocyclone-separation performance influenced by reflux device and different vortex-finder lengths, *Separation and Purification Technology*, *233*. (2020), p. 116013

[9] Xiong, Z., *et al.*, Development of a cyclone separator with high efficiency and low pressure drop in axial inlet cyclones, *Powder Technology*, *253*. (2014), pp. 644-649

[10] Duan, L., *et al.*, The flow pattern and entropy generation in an axial inlet cyclone with reflux cone and gaps in the vortex finder, *Powder Technology*, *303*. (2016), pp. 192-202

[11] Fu, S., *et al.*, Performance evaluation of industrial large-scale cyclone separator with novel vortex finder, *Advanced Powder Technology*, *32*. (2021), 3, pp. 931-939

[12] Guo, M., *et al.*, Numerical investigation on the swirling vortical characteristics of a Stairmand cyclone separator with slotted vortex finder, *Powder Technology*. (2023), p. 118236

[13] Pei, B., *et al.*, The effect of cross-shaped vortex finder on the performance of cyclone separator, *Powder Technology, 313*. (2017), pp. 135-144

[14] Misiulia, D., *et al.*, Effects of deswirler position and its centre body shape as well as vortex finder extension downstream on cyclone performance, *Powder technology, 336*. (2018), pp. 45-56

[15] Zhou, F., *et al.*, Experimental and CFD study on effects of spiral guide vanes on cyclone performance, *Advanced Powder Technology, 29*. (2018), 12, pp. 3394-3403

[16] Dasar, M.,R.S. Patil, Hydrodynamic characteristics of a 2D2D cyclone separator with a finned cylindrical body, *Powder Technology, 363*. (2020), pp. 541-558, DOI No. 10.1016/j.powtec.2020.01.021

[17] Yang, H.G., *et al.*, Effects of helical fins on the performance of a cyclone separator: A numerical study, *Advanced Powder Technology, 34*. (2023), 1, DOI No. 10.1016/j.apt.2022.103929

[18] Gao, Z., *et al.*, Time-frequency analysis of the vortex motion in a cylindrical cyclone separator, *Chemical Engineering Journal, 373*. (2019), pp. 1120-1131

[19] Cortes, C.,A. Gil, Modeling the gas and particle flow inside cyclone separators, *Progress in energy and combustion Science, 33*. (2007), 5, pp. 409-452

[20] Slack, M., *et al.*, Advances in cyclone modelling using unstructured grids, *Chemical Engineering Research and Design, 8*. (2000), 78, pp. 1098-1104

[21] Yao, Y., *et al.*, Effects of the inlet particle spatial distribution on the performance of a gas-solid cyclone separator, *Particuology*. (2023),

[22] Wang, B., *et al.*, Numerical study of gas–solid flow in a cyclone separator, *Applied Mathematical Modelling, 30*. (2006), 11, pp. 1326-1342

[23] Chu, K., *et al.*, CFD–DEM simulation of the gas–solid flow in a cyclone separator, *Chemical Engineering Science, 66*. (2011), 5, pp. 834-847

[24] Kumar, M., *et al.*, Dominant modes in a gas cyclone flow field using proper orthogonal decomposition, *Industrial & Engineering Chemistry Research*, 61. (2022), 6, pp. 2562-2579

[25] Dong, S., *et al.*, Experimental and numerical study on the performance and mechanism of a vortex-broken electrocyclone, *Chemical Engineering Journal*, 455. (2023), p. 140758

[26] Hu, L.Y., *et al.*, Studies on strongly swirling flows in the full space of a volute cyclone separator, *AIChE Journal, 51*. (2005), 3, pp. 740-749

[27] Hoffmann, A.C., *et al.*, Gas cyclones and swirl tubes: principles, design and operation, *Appl. Mech. Rev., 56*. (2003), 2, pp. B28-B29

[28] Avci, A.,I. Karagoz, Effects of flow and geometrical parameters on the collection efficiency in cyclone separators, *Journal of Aerosol Science, 34*. (2003), 7, pp. 937-955

[29] Yang, X., *et al.*, Effects of operational and geometrical parameters on velocity distribution and micron mineral powders classification in cyclone separators, *Powder Technology, 407*. (2022), p. 117609

Submitted: 27.05.2023
Revised: 26.07.2023
Accepted: 10.08.2023